International Journal of Automotive Technology, Vol. 5, No. 3, pp. 145–153 (2004)

1229–9138/2004/017–01

A PARAMETRIC SENSITIVITY STUDY OF GDI SPRAY CHARACTERISTICS USING A 3-D TRANSIENT MODEL

M. A. COMER[1], P. J. BOWEN[1]*, S. M. SAPSFORD[2] and S. I. KWON[3]

[1]Division of Mechanical Engineering, Cardiff University, Cardiff CF24 0YF, UK
[2]Ricardo Consulting Engineers Ltd., Shoreham-by-Sea BN43 5FG, UK
[3]Doowon Technical College, Ansung, Gyeonggi 456-890, Korea

(Received 28 January 2003; Revised 17 February 2004)

ABSTRACT–Potential fuel economy improvements and environmental legislation have renewed interest in Gasoline Direct Injection (GDI) engines. Computational models of fuel injection and mixing processes pre-ignition are being developed for engine optimisation. These highly transient thermofluid models require verification against temporally and spatially resolved data-sets. The authors have previously established the capability of PDA to provide suitable temporally and spatially resolved spray characteristics such as mean droplet size, velocity components and qualitative mass distribution. This paper utilises this data-set to assess the predictive capability of a numerical model for GDI spray prediction. After a brief description of the two-phase model and discretisation sensitivity, the influence of initial spray conditions is discussed. A minimum of 5 initial global spray characteristics are required to model the downstream spray characteristics adequately under isothermal, atmospheric conditions. Verification of predicted transient spray characteristics such as the hollow-cone, cone collapse, head vortex, stratification and penetration are discussed, and further improvements to modelling GDI sprays proposed.

KEY WORDS : GDI spray, PDA, VECTIS

NOMENCLATURE

A : radius of parent drop before undergoing breakup
n : droplet number
r : radius of new droplets produced after break-up of parent droplet
u : axial droplet velocity component
v : radial droplet velocity component
w : tangential droplet velocity component
D : droplet diameter
Re_D : droplet Reynolds number
r_i : radius of inner air core of spray at injector
r_o : radius of outer orifice of injector
V_{rel} : relative velocity of droplet to air
We_D : droplet Weber number
We_{Cr} : critical droplet Weber number
SOI : start of injection (from electronic signal, not first fuel to exit orifice)
σ_{liq} : surface tension of liquid
ρ_{gas} : density of gas
τ : characteristic time of droplet breakup
ν_l : kinematic viscosity of liquid
ϕ_i : swirl angle at inner surface of spray cone at injector orifice
ϕ_o : swirl angle at outer surface of spray cone at injector orifice

*Corresponding author. e-mail: BowenPJ@cf.ac.uk

1. INTRODUCTION

Gasoline Direct Injection (GDI) is regarded as one of the most promising methods for reducing fuel consumption of spark ignition (SI) engines. GDI engine designs commonly utilise pressure swirl injectors as the means of fuel delivery (Harada *et al.*, 1997; Iwamoto *et al.*, 1997; Ohsuga *et al.*, 1997), and vary injection timing between late (stratified charge) for low speed and part load operation, and early (homogeneous charge) for high load operation. These two modes of operation have different fuel spray characteristic requirements. Early injection (low ambient pressure/temperature) requires a widely spread fuel spray to form a homogenous mixture, whilst minimising piston/liner wall wetting which results in soot production. Late injection (high ambient pressure/temperature) requires a compact spray with well atomized fuel, which can vaporize in the short time before ignition. The sprays produced by pressure swirl atomizers are affected by the ambient pressure such that higher pressures are claimed to result in narrower spray cone angles and

reduced penetration, rendering them potentially suitable for use in GDI engines (Kume *et al.*, 1998). The commercial injector used in this study is representative of those proposed for use in GDI engines.

The application of numerical models to the prediction of fuel and charge flows within the cylinder of GDI engines can potentially reduce design analysis work and unnecessary costly production of non-optimised engine components. Two-phase numerical spray models suitable for engine applications have been developed over the last 15 years or so. However, these models have only been verified against limited data sets, due to the difficulty in providing suitable spatially and time resolved experimental data. Previously, Comer *et al.* (1999) discussed the provision of such data and demonstrated the suitability of post-processed Phase Doppler Anemometry (PDA) data to provide spatially and time resolved spray characteristics comprising particle size, three velocity components and fuel mass indicators in the open atmosphere under low purge rate.

The aim of this study is to compare and appraise numerical predictions from a 3-D two-phase Euler-Lagrangian spray model against this comprehensive data set. In the absence of geometrical injector specifications, the approach adopted is to estimate global injector characteristics such as orifice size, cone angle and mass flow profile from independent experimental diagnostic studies, and then to conduct a parametric sensitivity study on the effects of swirl, comparing predictions against downstream characteristics. Primary atomisation is not within the scope of this study. A systematic procedure is proposed for selection of appropriate input parameters to enable downstream modelling of a spray produced by a pressure swirl atomizer suitable for use in GDI engines. This study in the 'open' atmosphere is required before progressing towards appraising the model's predictive capability in engine-type environments, i.e. raised temperature and pressure. Future model developments are suggested.

2. EXPERIMENTAL CHARACTERIZATION

As the time-resolved PDA methodology has been previously reported in detail (Comer *et al.*, 1999), only a brief resume is included in this section. Other independent experimental studies required to provide initial boundary conditions for model input are also summarised.

2.1. Fuel Injection Rate

A representation of the transient mass flow rate signature is one injector characteristic required to initialise the numerical model; this is not available from the injector manufacturer, and so a suitable experimental programme was undertaken to provide an approximation for this diagnostic profile. The injector was operated at a line pressure of 10 MPa and a pulse duration of 1.5 ms, which resulted in a total mass of approximately 10 mg being discharged per injection. Line pressure was measured during one injection to assist in defining the mass flow rate characteristic. A transducer was mounted immediately upstream of the injector, and approximately 200 mm from the orifice. The resulting pressure trace is shown in Figure 1.

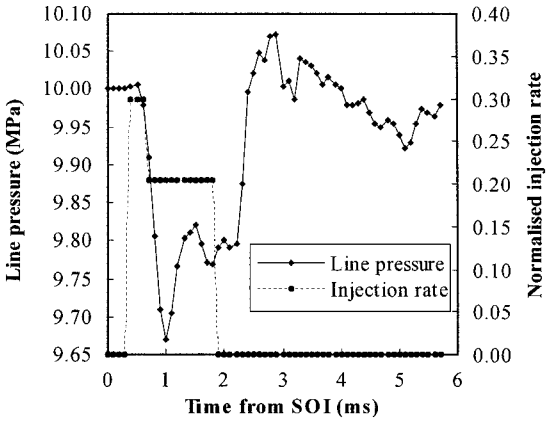

Figure 1. Characterisation of line pressure transient during injection.

There is a delay of approximately 0.5 ms after the start of injection (SOI), which is attributable to the electro-mechanical delay of the injector and the time taken for the pressure to drop through the injector, before a reduction in the line pressure. Previous studies (Comer *et al.*, 1999) have shown the time taken for fuel to emerge from the orifice to be of the order of 0.3 ms. The initial pressure drop coincides with the injection of a 'slug' or 'pre-spray' of fuel. This has been witnessed by the authors for this particular injector, as well as by other investigators studying pressure swirl atomizers (Parrish *et al.*, 1997; Stanglmaier *et al.*, 1998; Shelby *et al.*, 1998; Hoffmann *et al.*, 1998), and is thought to be caused be the rapid emptying of the sac volume. This phase of injection is proceeded by a steady phase, when the fuel exiting the injector forms a hollow cone following stabilisation of flow within the injector.

These two phases of injection can be identified on the pressure trace as the initial 'trough', and subsequent quasi-stable section of the trace, which oscillates around 9.8 MPa. As a first approximation for modelling purposes, the flow was divided into an early region of higher flow from 0.3 to 0.6 ms, followed by a period of reduced flow until the end of the injection. A 3:2 ratio for flow rates in the two periods is specified, from which flow rates of 9.1 and 6.06 mg/ms respectively are derived. The 0.3 ms delay at the start is intended to simulate the electro-mechanical delay.

2.2. High Speed Ciné Photography

Spray cone angle is another feature of injector performance required before modelling can commence. This parameter was determined via high-speed cine photography, which was also used to consolidate some of the global spray features identified in the PDA characterisation, such as penetration and the transient development of the head vortex.

A Photo high speed camera, with film speeds operating up to 10,000 frames per second and illumination by a synchronised laser sheet from a 5 W Copper vapour laser, was utilised to provide this data.

2.3. Time-resolved Phase Doppler Anemometry (PDA)

An experimental grid of 143 measurement points extending 90 mm axially and 28 mm radially, comprising one half of the spray, was traversed. At each point, droplet size and 2 components of velocity (axial and radial) were measured. By rotating the injector and measurement plane through 90°, it is possible to obtain the third component of velocity (swirl), and a second set each of axial velocity and droplet size at each point. The injector operated at a line pressure of 10 MPa and a pulse period of 1.5 ms, injecting into ambient air. An injector frequency of 4 Hz ensured no interference between successive sprays (Comer *et al.*, 1999). Data from 15000 droplets were collected at each point. The data collection system timed out after 75 seconds if insufficient data had been collected by this time. The data corresponding to each grid point was then divided into 25 time bins for droplets arriving before 12 ms, and grouped into global time bins enabling phase averaged flow field and droplet size plots to be derived. These plots are now used for verification of the model predictions.

3. NUMERICAL MODEL

VECTIS is a CFD suite of modules developed by Ricardo Consulting Engineers Ltd. for analysis of engine-related problems. It solves the conservation equations of mass, momentum, energy and chemical species, and models turbulence using the k-ε model. It also has a spray module which can perform transient modelling of dispersed phases in a continuous fluid phase (Ricardo, 2000).

The spray module uses a Lagrangian stochastic formulation applied to parcels of dispersed phase droplets, which each contain many droplets of equal size, velocity and temperature. The droplets and the continuous phase interact through fluid dynamic and heat and mass transfer, resulting in changes to the size, velocity and temperature of the droplets, and pseudo-simultaneous changes in the continuous phase. Model parameters comprise initial droplet size distribution, injection rate, break-up

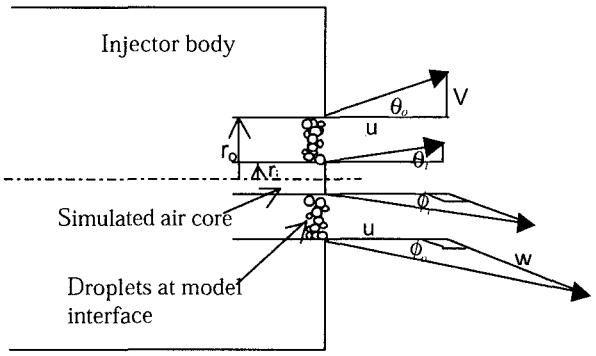

Figure 2. Model parameters representing orifice conditions.

model (if required), droplet interactions with other droplets and turbulence. A study of the relative influence of these input parameters is discussed later.

3.1. Model Initial and Boundary Conditions

A characteristic of pressure swirl atomizers is that during stable flow conditions, the fuel exits the orifice as a swirling, annular liquid sheet, with the centre part of the orifice occupied by an air core (Chinn *et al.*, 1997). The dimensions of the air core are difficult to ascertain experimentally on injectors of this scale, and their measurement remains an active area of research. The existence of the core may be simulated in the current model by specifying an inner orifice radius r_i (Figure 2).

For a given mass flow rate, the axial velocity, and hence penetration of droplets exiting the injector, will be necessarily higher for larger inner radii. The orifice of the injector tested has an outer radius (r_o) of approximately 170 μm, with the inner radius set to 50 mm. Droplet/turbulence interactions have been included, but interactions between droplet parcels have not, as there is little evidence to date to support coalescence of droplets in the swirling sprays produced by pressure swirl atomizers operating at atmospheric pressure.

The fuel exiting the orifice of a pressure swirl injector is thought to be made up of a thin annular sheet, ligaments and droplets. The break up length of the sheet and ligaments for these injectors (<10 mm), alongwith the density of the spray, account for reduced PDA validation rates in the near orifice region (Wigley *et al.*, 1998). While models of primary atomisation should be sought, in the context of engine modelling, the purpose of fuel spray modelling is ultimately to predict the behaviour of the droplets downstream of the injector. Hence numerical model requires a size probability density function (PDF) for droplets introduced. The injection process is divided into discrete phases as described in section 2.1. For each phase, a relatively simple PDF correlated with the global average diameter size D_{10} (=Σ

n_iD_i/n_i) at the end of the injection derived from the PDA data is used for to characterise initial droplet sizes. During each phase, a finite number of discrete droplet parcels are introduced at the injector, and from the mass injection rate and nozzle diameter, the droplets exit velocity during each phase is calculated. Validated empirical global particle size correlations could also be utilised to obtain the initial PDF, although such correlations have not been utilised in this study. Inner and outer cone angles (θ_i and θ_o respectively) are specified in the model as half angles. The angle is varied linearly between the two extremes. The outer cone half angle is measured from the ciné film to be approximately 25° for this particular injector.

Modelling swirl flow from an injector is facilitated by the addition of a tangential velocity component of the exiting fuel. Swirl is defined as an angle ϕ at the inner and outer radii of the orifice, and is varied linearly between these two points.

$$\tan(\phi)=\text{tangential velocity(w)/axial velocity(u)} \quad (1)$$

Droplet parcels are introduced randomly across the model orifice interface and assume axial, radial and tangential velocities as specified by the relevant angles at their point of entry. Chinn & Yule (Chinn *et al.*, 1997) have modelled the internal flow of a pressure swirl injector, and have noted the existence of a hybrid 'Rankine' vortex for the profile of the tangential (swirl) velocity. Their analysis predicts a greater tangential velocity near the orifice centre, due to the solid body rotation of the air core, with a smooth transition to the free-vortex in the outer area of flow. The PDA data consolidates this phenomenological picture, particularly during the stable phase.

3.2. Secondary Atomization Models

This study utilises two droplet break-up models : Reitz & Diwakar (Reitz *et al.*, 1986), and the wave model of Liu *et al.* (1993). The first assumes that a droplet can undergo two types of breakup. 'Bag' breakup occurs when the droplet Weber number (We_D) is greater than a predefined critical value (We_{Cr}), where :

$$We_D=\rho_{gas}\, V_{rel}^2 D/\sigma_{liq} \geq We_{Cr}=12 \quad (2)$$

Stripping break-up is believed to be caused by Kelvin-Helmholtz surface waves, and occurs for droplet Weber numbers much higher than those associated with the bag-breakup limit. The following correlation has been proposed for this category of droplet breakup mechanism :

$$We_D/Re_D^{1/2} \geq 0.5 \quad (3)$$

where

$$Re_D=V_{rel}D/\nu_l \quad (4)$$

The wave model of Lui *et al.* (1993) assumes that droplet surface wave perturbations have maximum growth rates and wavelengths related to the properties of the dispersed and continuous phases. Secondary atomisation of parent droplets by 'stripping' break up results in new droplets of radius r, and a corresponding reduction in the radius of the parent drop (a) following the equation :

$$da/dt=-(a-r)/\tau \quad (5)$$

where τ is the time taken for a droplets to reach a stable size.

For representative purposes, the first model predicts that relative velocities in excess of 100 m/s for 'bag' break-up, and 200 m/s for 'stripping' break-up, would be required for droplets of 20 μm – the largest d_{10} measured in the spray – to undergo break-up under atmospheric conditions. PDA results indicate that the first droplets emitted have maximum velocities in the region of 60 m/s. Average velocities of 100 m/s are measured about 1 ms after SOI, but are injected into air which is moving due to the momentum exchange of the preceding droplets, and therefore relative velocities are reduced. Hence, it is unlikely that secondary droplet break-up will play a significant role in the modelling of the fuel spray.

3.3. Spatial and Temporal Discretisation

Fuel sprays are modelled in a constant volume cuboid with 100 mm vertices. The injector orifice is positioned at the centre of one face, and the spray injects vertically downwards. Two areas of increased cell density centred on the spray axis are employed. A grid sensitivity study demonstrates the influence of grid cell density on the accuracy of solution. Figure 3 shows the general form of the grid with dimensions at refinement block boundaries given in millimetres. Details of the number of cells in the refinement blocks for the three test cases are specified in Table 1. The models were run on a Silicon Graphics Origin 2000 6-processor system.

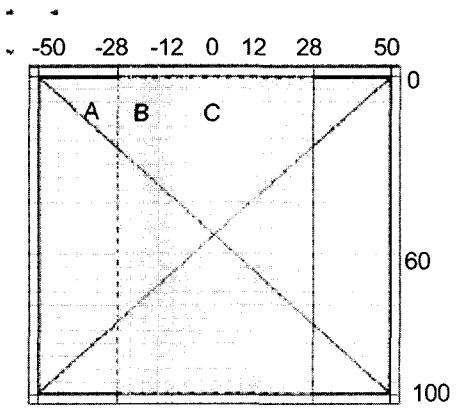

Figure 3. Schematic of numerical grid.

Table 1. Computational grids used in grid sensitivity study.

	Case1	Case 2	Case3
	Fine	Medium	Coarse
Block B cell side length	1 mm	2 mm	4 mm
Block B number of cells	279040	34880	4360
Block C cell side length	0.5 mm	1 mm	2 mm
Block C number of cells	276480	34560	4320
Total number of cells (incl. A)	566865	75113	11630

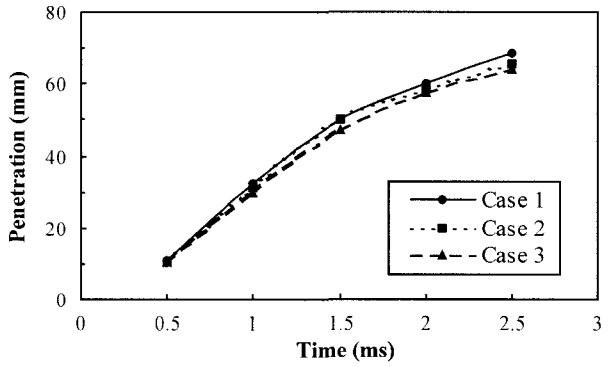

Figure 4. Effect of spatial grid refinement on penetration.

Figure 4 shows the penetration profiles predicted by the three cases. It is evident that all three predict very similar penetration profiles, although case 3 under predicts the other two cases somewhat after 0.5 ms. By 2.0 ms after SOI, case 2 under predicts case 1 by 2 mm,whilst employing almost an order of magnitude fewer cells, with a corresponding reduction in run time.

A similar sensitivity study has been undertaken to establish an appropriate time-increment which provides suitable compromise between solution accuracy and run-time required for convergence. Predictions have been compared utilising time increments ranging from 100 down to 2.5 μs until 3 ms after SOI, effectively decreasing the Courant number and hence reducing numerical dispersion. This range of time increments resulted in an order of magnitude increase in run times. For larger Courant numbers (Cr), the spray cone diverged indefinitely with no indication of cone collapse, whilst employing a time increment of 10 μs (Cr<1), the solution converges to a satisfactory tolerance in terms of penetration, and droplet size distribution within the spray. However, a conservative time increment of 5 μs was employed for all the further predictions presented, to ensure Courant convergence in all case studies presented. This value is also consistent those utilised by other researchers investigating similar problems (Lui *et al.*, 1997; Han *et al.*, 1997).

3.4. Model Appraisal Approach

The sensitivity of the predictions relative to numerical discretisation has been discussed earlier, and all further results presented are for the optimised schemes, i.e. case 2 spatial grid with a time step of 5 μs. Three injector characteristics, cone angle, mass flow and initial particle size are determined from relatively straightforward injector diagnostic measurements, namely photography, fuel-line pressure and a spatially and time averaged mean particle size - in this case derived from the PDA data set. A parametric sensitivity study is undertaken on the remaining parameter, swirl angle, and the type of secondary break-up model employed, although as reasoned in the previous section, secondary break-up is not expected to have a dominant influence. It is important to note that no other form of model tuning has been employed. The predictions are compared with field characteristics from the PDA data-set such as spatial distribution of droplet sizes, axial radial streamlines, collapse of the 'hollow' cone, and entrainment characteristics. To provide the best representation of the experimental initial conditions, the swirl angle is first approximated from the third velocity component (swirl) derived from the time-resolved PDA measurements near the injector, and downstream spray predictions are then compared against downstream spray characteristics.

4. RESULTS & DISCUSSION

4.1. Effect of Swirl on Model Predictions

Figure 5 contains model predictions for three cases, with injector swirl angle being the only variant. Each plot shows a 5mm slice through the centre of the spray, with velocity vectors in the upper half, and mean droplet size in the lower half. The predictions are plotted 1.625 ms after SOI, about the time when the final fuel is being discharged, allowing for electromechanical delay. Grid lines are spaced at 5 mm intervals in both directions.

Figure 5(a) shows predictions when the swirl velocity component is set to zero. The model predicts the spray to have penetrated 60 mm downstream, the spray cone envelope is almost parallel after 15 mm, entrainment is very low and there is only a minimal hollow feature of the spray. It should be noted that the 'hollow' cone is not apparent in the predictions even though an inner cone angle has been specified. Figure 5(b) shows predictions when inner and outer swirl angles are set at 10°. The spray has broadened and penetration is reduced. It is starting to develop the characteristic 'hollow' core, entrainment rates are starting to increase, and the spray is showing more evidence of size stratification across the cone radius. Figure 5(c) has both inner and outer swirl

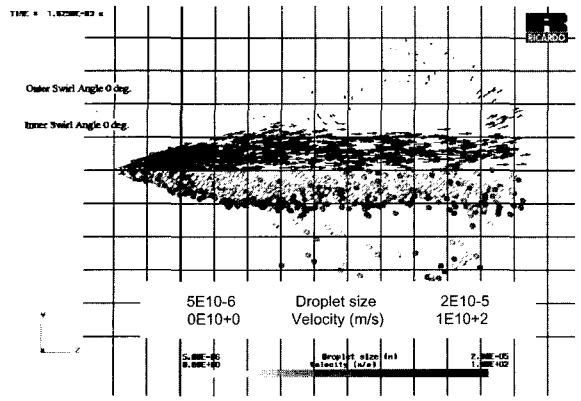

(a) Swirl angle 0 deg.

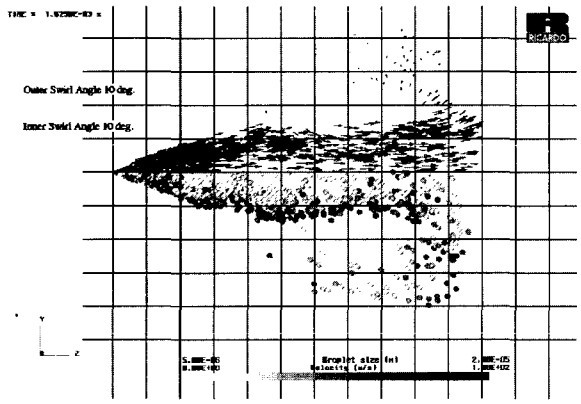

(b) Swirl angle 10 deg.

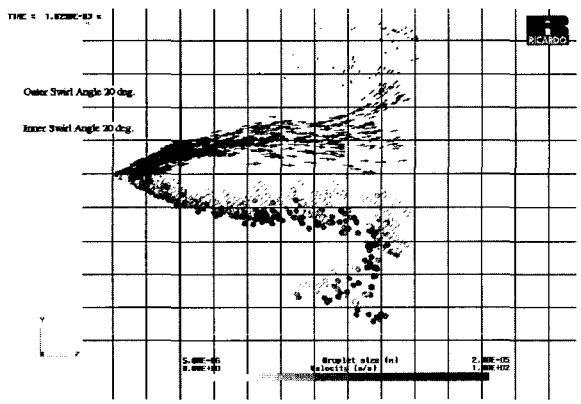

(c) Swirl angle 20 deg.

Figure 5. VECTIS predictions 1.625 ms after SOI.

angles set at 20°. Penetration is reduced further, and most of the spray is now concentrated in a spray annulus some 4–7 mm thick, with the smaller droplets (<5 μm) residing within the inner section, and larger (8~12 μm) droplets, representing the majority of the mass, dominating the outer regions; as to be expected from centrifugal effects. Cone angle at the base of the spray has also increased, suggesting that this may need consideration when specifying the input cone angle.

4.2. Effect of Break-Up Model

The plots presented in Figure 5 are all produced using the Reitz-Diwakar break-up model. Analysis of the spray in Figure 5 was also performed using the model of Liu *et al.* (1993). In both cases stripping type break-up affected less than 30 droplet parcels from 5000. This suggests that at these operating conditions, the models behave in a similar manner, and both correctly predict that there is minimal secondary atomization, which is confirmed by the PDA data.

4.3. Model Verification

Figure 6 presents processed PDA data for the time bin 1.5 to 1.75 ms after SOI and the VECTIS predictions for nominally the same time (1.626 ms after SOI). The upper graph contains velocity vectors for the in-plane components and line diagrams indicating through-plane (swirl) velocity. The central graph presents the VECTIS predictions when swirl angles are set to 20 degrees, with the upper half and lower halves representing the velocity and droplet-size fields respectively. The lower plot provides contour plot of PDA-measured mean diameters (D_{10}). 'Holes' in the plots indicate that fewer than 10 droplets were sampled at those points within this particular experimental time bin, which is evidence of the hollow cone characteristic of this injector.

It can be seen from experimental data that the greatest velocities exist in the near orifice region, and persist through the centre of the spray. A head vortex is present approximately centred at the 35 mm/12 mm axial/radial position.

The areas of highest mass flow comprise droplets with D_{10} between 8 and 12 μm. Penetration measured from the ciné images indicates the head of the spray at 40 mm, and the early slug tip at around 50 mm, 1.625 ms after SOI. The early fuel 'slug' is not considered in this study, and so the experimental value for penetration is considered to be 40 mm at this instant after SOI.

It is noted from Figure 5 that predictions for 20° swirl angle presents predictions for the case corresponding to the best estimate for experimental initial conditions. Penetration and head vortex position are accurately predicted, as indicated by comparing the top-halves of the upper two graphs in Figure 6. The location of the high-mass flow region is modelled extremely well, as is the extent of core hollowness and position of core collapse, as indicated by comparing the lower-halves of the lower two plots in Figure 6. Droplet size stratification across the cone radius is less evident in the d_{10} plot comparing data with prediction in Figure 6, but Sauter mean diameter

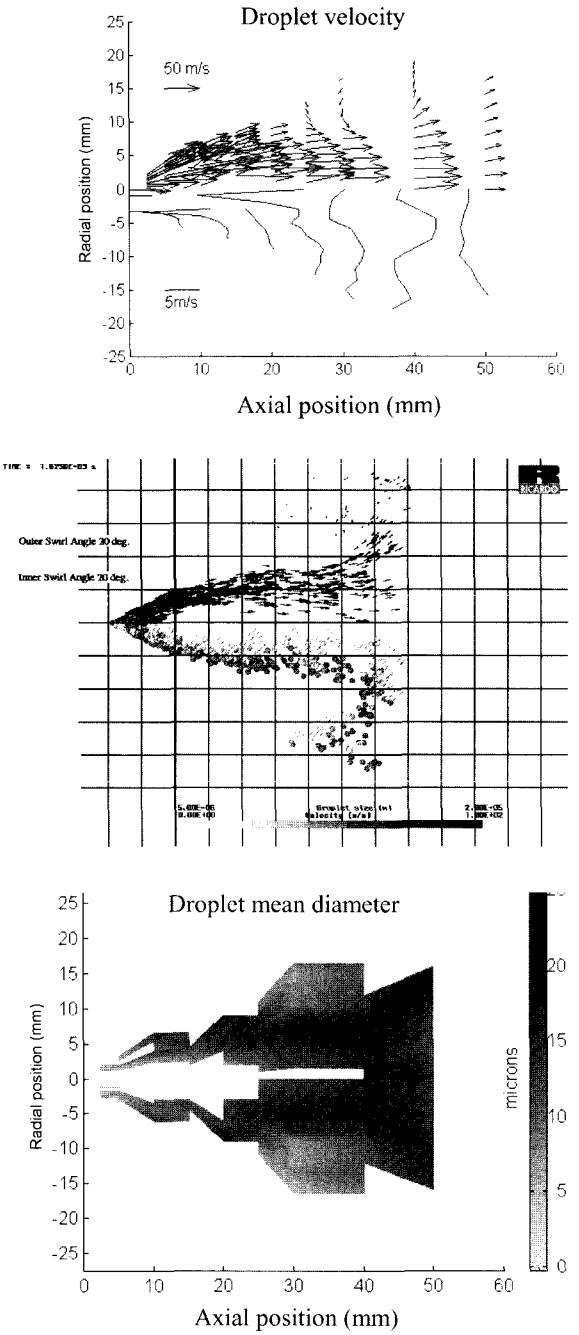

Figure 6. VECTIS/PDA comparison nominally 1.625 ms after SOI: Upper - velocity-field; Lower-droplet-size field.

plots of the same spray do show larger sizes to the outer edge (Comer *et al.*, 1999).

4.4. Model Predictions of Transient Spray Development

Figure 7 presents a full sequence of model predictions at discrete moments after SOI for the case utilising 20° swirl angle, i.e. the optimised conditions. The initial well-defined cone angle is self-evident in Figure 7(a), some 0.375 ms after SOI, i.e. just after the injection delay due to electromagnetic response. There is no particular structure of note within the spray core at this stage. Half a milli-second later (Figure 7b), several features characterised in the experimental studies are developing. The functional relationship between cone angle and time is apparent, as the border of the spray projects a curved trajectory. In the centre, the swirl component facilitates the development of the hollow core which is now clear, and stratification effects are evident as smaller droplets get drawn into the low pressure central region, whereas the larger droplets continue their helical paths at wider cone angles due to relative momentum effects. The leading spray front, which is progressing into the pseudo-stagnant flowfield ahead of the spray, has initiated development of the head vortex characteristics, diagnosed by an increase in positive, and appearance of negative, radial velocity components. This aids entrainment of ambient air, and hence dilutes the fuel rich spray cone. The head vortex is developing 25–30 mm downstream, which concurs with the laser diagnostic studies. By the next time instant selected (1.375 ms after SOI – Figure 7(c), these features are consolidated and established. Inner streamlines show a parabolic variation from the injector orifice to the collapse of the hollow core about 35 mm downstream. The fuel mass is concentrated with a thin 4–7 mm annulus until breakdown of the core. Whereas stratification is clear within the fuel annulus, a range of droplet sizes populate the head vortex, which has broadened radially. The spray is very well established at this stage, during the central period of injection. All these features are fully consistent with the picture presented by the experimental data-set. By 1.875 after SOI, the pintle has closed, diagnosed by the 5 mm progression of the spray tail from the orifice exit. The spray has retained its hollow structure, which progresses systematically downstream. The outlying droplets which have been forced radially outwards initially before re-entrainment, extend some 30 mm from the centreline in the later time plots (Figure 7d-f), whilst the spray as a whole continues to progress axially at about 30 m/s.

Modelling the early 'slug', which is characterised by larger droplets with little swirl, should be considered in future programmes. Reducing the outer swirl angle for more consistency with the exiting Rankine vortex may also be considered for future sensitivity studies, although these results suggest that this should have only a secondary influence. Finally, the experimental and numerical modelling approaches adopted have been shown to be complimentary, and provide confidence in progressing the work programme onto conditions of elevated temperatures and pressures more representative of those pertaining in-cylinder.

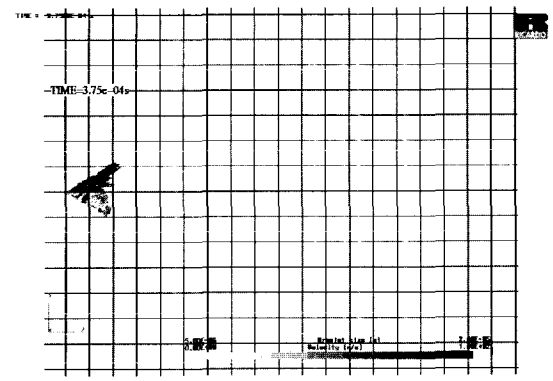

(a) Time=0.375 ms after SOI

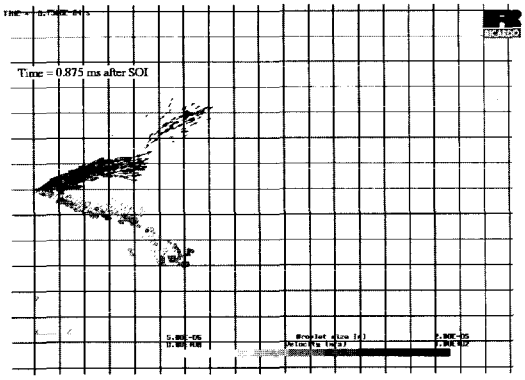

(b) Time=0.875 ms after SOI

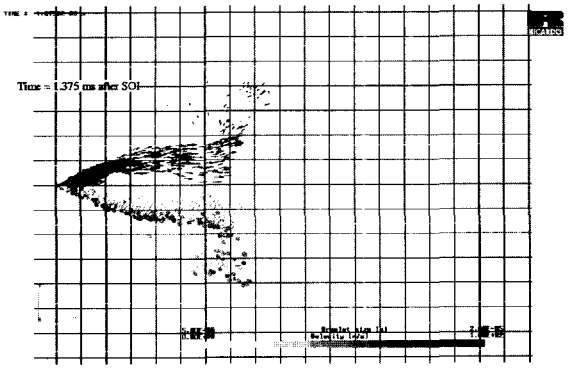

(c) Time=1.375 ms after SOI

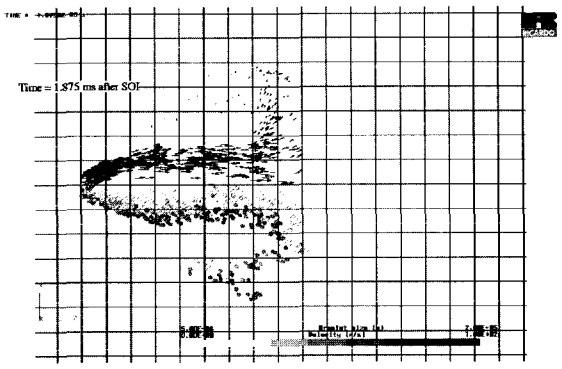

(d) Time=1.875 ms after SOI

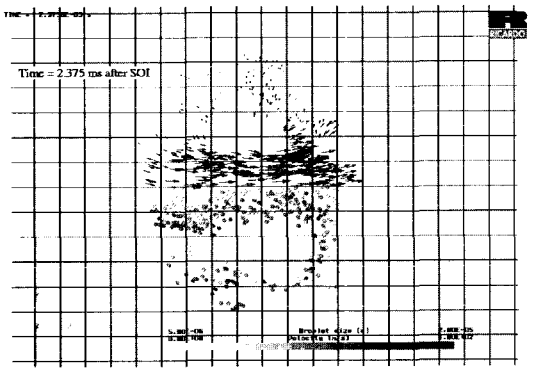

(e) Time=2.375 ms after SOI

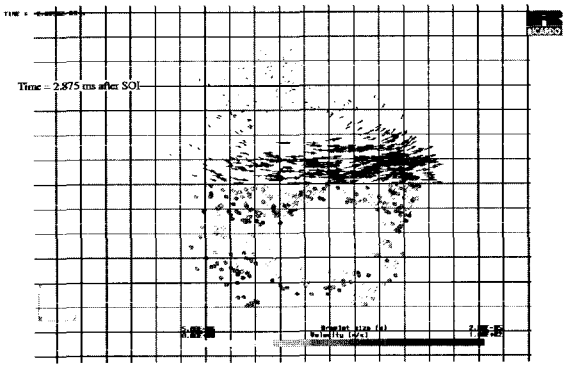

(f) Time=2.875 ms after SOI

Figure 7. Sequence of transient model predictions for spray duration.

5. CONCLUSIONS

(1) In the absence of detailed injector design information, a minimum of 5 primary injector parameters are shown sufficient to model primary characteristics of GDI sprays downstream using the two-phase numerical model VECTIS. These parameters are: (i) cone angle close to the injector; (ii) injector orifice size; (iii) a global measure of d_{10}; (iv) injection mass and rate signature, simplified perhaps to a two-step injection rate diagram; and crucially; and (v) a measure of swirl, which may be modelled adequately by an exiting swirl angle.

(2) Comparison of temporally measured and predicted detailed spray characteristics for a GDI pressure-swirl injector has been undertaken through analysing

diagnostics such as droplet velocity profiles, axial-radial streamlines, penetration, head-vortex characteristics, extent of hollowness and mass distribution. In general, reasonable agreement has been noted between data and predicted values. However, the predictions currently exaggerate droplet-size stratification across the thin spray wall.

(3) The critical influence of swirl (introduced via a swirl angle) is highlighted for the first time, showing in particular its dramatic impact on the size and extent of the hollow cone, and the temporal development of the head vortex.

(4) Improvements to the overall modelling of the injection process could be achieved by modelling the injection of the initial 'slug' of fuel, which has primarily axial velocity, and the pintle bounce after the main injection. Both events were identified during the time-resolved PDA technique and cine film studies, and both are important for prediction of overall engine efficiency. An improved method for characterising the injection rate other than the two-step approximation utilised here should also be considered.

(5) Input conditions required for this numerical model suggest that there is scope for future consideration of linking models of internal injector flow with downstream spray characteristics to reduce further the number of parameters required for GDI spray predictions.

ACKNOWLEDGMENTS–The authors would like to thank the Directors of Ricardo Consulting Engineers Limited for their financial support and permission to publish this paper. Financial support for Martin Comer in the form of an EPSRC studentship under the Total Technology Scheme is also gratefully acknowledged. The award of a Joint Research Equipment Initiative UK EPSRC grant to purchase the Origin 2000 Silicon Graphics computer which facilitated the computational study is gratefully acknowledged. Finally, helpful discussions with other Ricardo engineers and management staff including Melanie Sadler, Simon Edwards, Neville Jackson and Martin Gold during the period of study have been very helpful and greatly appreciated.

REFERENCES

Chinn, J. J. and Yule, A. J. (1997). Computational analysis of swirl atomizer internal flow. *Proc. ICLASS 97*, Seoul, Korea, 868–875.

Comer, M. A., Bowen, P. J., Sapsford, S. M., Bates, C. J. and Johns, R. J. R. (1999). Transient 3D analysis of a DI gasoline injector spray. *Journal of Atomisation and Sprays* **9**, 467–482.

Han, Z. and Reitz, R. D. (1997). Internal structure of vaporising pressure-swirl fuel sprays. *Proc. ICLASS 97*, Seoul, Korea, 474–481.

Harada, J., Tomita, T., Mizuno, H., Mashiki, Z. and Ito, Y. (1997). Development of direct injection gasoline engine. *SAE Paper No.* 970540.

Hoffman, J. A., Khatri, F., Martin, J. K. and Coates, S. W. (1998). Mass-related properties of atomizers for direct-injection SI engines. *SAE Paper No.* 980500.

Iwamoto, Y., Noma, K., Nakayama, O., Yamauchi, T. and Ando, H. (1997). Development of gasoline direct injection engine. *SAE Paper No.* 970541.

Kume, T., Iwamoto, Y., Iida, K., Murakami, M., Akishino, K. and Ando, H. (1998). Combustion control technologies for direct injection SI engine. *SAE Paper No.* 960600.

Liu, A. B., Mather, D. and Reitz, R. D. (1993). Modelling the effects of drop drag and breakup on fuel sprays. *SAE Paper No.* 930072.

Lui, Z., Lin Y., Arai M., Obakata T. and Reitz R. D. (1997). Numerical study of liquid spray characteristics. *Proc. ICLASS 97*, Seoul, Korea, 804–811.

Ohsuga, M., Shiraishi, T., Nogi, T., Nakayama, Y. and Sukegawa, Y. (1997). Mixture preparation for direct-injection SI engines. *SAE Paper No.* 970542.

Parrish, S. E. and Farrell, P. V. (1997). Transient spray characteristics of a direct-injection spark-ignited fuel injector. *SAE Paper No.* 970629.

Reitz, R. D. and Diwakar, R. (1986). Effect of breakup on fuel sprays. *SAE Paper No.* 860469.

Ricardo Software. (2001) VECTIS Computational fluid dynamics users manual. Version 3.5. *Ricardo*. London.

Stanglmaier, R. H., Hall, M. J. and Matthews, R. D. (1998). Fuel-spray/Charge motion interaction within the cylinder of a direct-injected, 4-valve, SI engine. *SAE Paper No.* 980155.

Shelby, M. H., VanDerWege, B. A. and Hochgreb, S. (1998). Early spray development in gasoline direct-injected spark ignition engines. *SAE Paper No.* 980160.

Wigley, G., Hargrave, G. K. and Heath, J. (1998). A High power, high resolution LDA/PDA system applied to dense gasoline direct injection sprays. *Proc.* 9th *Int. Symp. on Applications. of Laser Techniques to Fluid Mechanics* Lisbon, 9.4.1 9.4.7.